Hindawi

Research Article

Particle Ratios in a Multicomponent Nonideal Hadron Resonance Gas

Rameez Ahmad Parra [1], **Saeed Uddin** [2], **Waseem Bashir** [3], **and Inam-ul Bashir** [4]

[1]*Department of Physics, Central University of Kashmir, India*
[2]*Department of Physics, Jamia Millia Islamia (Central University), New Delhi, India*
[3]*Department of Physics, Government Degree College, Budgam, J&K, India*
[4]*Jammu & Kashmir, Higher Education Department, India*

Correspondence should be addressed to Rameez Ahmad Parra; rs.rameezparra@jmi.ac.in

We have considered formation of a multicomponent nonideal hot and dense gas of hadronic resonances in the ultrarelativistic heavy ion collisions. In the statistical thermal model approach, the equation of state (EoS) of the noninteracting ideal hadron resonance gas (IHRG) does not incorporate either the attractive part or the short-range repulsive part of the baryonic interaction. On the other hand, in the nonideal hadron resonance gas (NIHRG) model, we can incorporate these interactions using the van der Waals (VDW) type approach. Studies have been made to see its effect on the critical parameters of the quark-hadron phase transition. However, it can also lead to modifications in the calculated relative particle yields. In this paper, we have attempted to understand the effect of such van der Waals-type interactions on the relative particle yields and also studied their dependences on the system's thermal parameters, such as the temperature and baryon chemical potential (μ_B). We have also taken into account the decay contributions of the heavier resonances. These results on particle ratios are compared with the corresponding results obtained from the point-like, i.e., noninteracting IHRG model. It is found that the particle ratios get modified by incorporating the van der Waals-type interactions, especially in a baryon-rich system which is expected to be formed at lower RHIC energies, SPS energies, and in the forthcoming CBM experiments due to high degree of nuclear stopping in these experiments.

1. Introduction

The particle production in the hot and dense hadronic medium created in the ultrarelativistic heavy ion collisions enables us to understand the final stage properties of such a hadronic matter. The matter which existed at the very early stages of universe can be recreated and studied in these collisions, though at a very small length scale. It is believed that the matter created in such nuclear collisions in the laboratory can achieve reasonably high degrees of thermal and chemical equilibrium. The study of the hadronic yields in the heavy ion collisions at ultrarelativistic energies is therefore an important tool to explore the properties of the hadronic matter, also called fireball, formed in these collisions [1–10].

The statistical thermal models provide a suitable framework to study the final stage properties of the hot fireball formed in the ultrarelativistic nucleus-nucleus collisions [11–20]. The hot and dense secondary partonic matter (consisting of quarks and gluons) initially produced within the fireball is in a preequilibrium state. These secondary partons continue to undergo multiple elastic and inelastic collisions. The fireball initially formed in the collision thus grows in size due to multiparticle production. It also simultaneously develops a hydrodynamic expansion due to the collective effect. The system thus reaches a state of sufficiently high degree of thermal and chemical equilibrium with sufficiently large number of particles within it which then permits the application of the statistical thermal models. If the initial temperature (T) and net baryon density

(ρ) is sufficiently high, i.e., $T > T_C$ (or $\rho > \rho_C$), then this may result in the formation of quark gluon plasma (QGP) phase [21–24]. This state is then followed by a mixed phase of QGP+HRG, assuming a first-order phase transition. After the completion of a first-order phase transition process, the particles (i.e., the hadrons) in the HRG phase still continue to interact. The collisions among the produced hadrons can lead to a high degree of thermal and chemical equilibrium of various hadronic species in the HRG phase as well. The HRG system continues to grow, expand, and cool and in the process gets diluted. After this, a freeze-out occurs when the mean free paths of these particles become comparable with the overall size of the system [25–28].

It has been highlighted earlier that the point-like hadrons do not reproduce the ground state properties of the nuclear matter. Further, no reasonable first-order QGP–HRG phase transition within the framework of a thermal model can be constructed with suitably large number of degrees of freedom in the HRG phase [29–32]. This essentially happens because a large number of point-like hadronic resonances can be thermally excited at high temperatures in absence of any repulsive interaction in a given physical volume of the system. Consequently, at adequately high temperature, the pressure in the ideal HRG phase pressure becomes more than the pressure in the QGP phase (i.e., $P_{HRG} > P_{QGP}$). Or in simple words, considering a first-order quark-hadron phase transition in a statistical thermal model framework with sufficiently large number of hadronic degrees of freedom, the system at high temperatures reverts to the hadronic resonance gas (HRG) phase [33–37]. According to lattice quantum chromodynamics (LQCD) predictions for vanishing net baryon number, the phase transition occurs at the critical temperature around 160 MeV and the system remains in the QGP phase at further higher temperatures [38–40]. Therefore, the result obtained by considering the HRG system consisting of point-like hadrons contradicts the LQCD prediction. However, within the framework of the statistical thermal models, this problem can be solved by considering the repulsive interactions between baryons (or antibaryons), which give rise to an excluded volume type effect. Moreover, in some phenomenological models, the attractive and repulsive interactions both have been taken into account where the strength of the repulsive interaction is proportional to the net baryon number density (n). Consequently, this interaction ceases to exist for $n \cong 0$ [41–43]. We have employed grand canonical ensemble (GCE) partition function approach to describe the properties of a gas of interacting hadronic resonances. The canonical ensemble partition function approach does not give broad thermodynamical picture of the hadronic system, because the number of particles and total energy is usually not conserved in the real physical systems formed in the ultrarelativistic nuclear collisions. The interactions in the multicomponent hadron resonance gas (HRG) can be incorporated in a more appropriate way by using the grand canonical ensemble (GCE) partition function approach. The repulsive part of interaction has been earlier incorporated through an excluded volume type effect in the HRG model

and is generally known as EV-HRG model of heavy ion collisions [44–46]. On the other hand, the attractive part of interaction is incorporated by way of multiplying the grand partition function with an exponential factor containing an average attractive potential. The attractive and repulsive interactions can be incorporated by other ways also, such as in the nonlinear Walecka model and its generalizations [47–51]. In case of the classical van der Waals-type approach, the strength of repulsion is proportional to the total particle density and is therefore finite even at zero baryon chemical potential ($\mu_B = 0$). Conversely, in the case of the Walecka model, the strength of repulsion is proportional to the *net* baryon density, and hence, it vanishes at $\mu_B = 0$. This is therefore a significant advantage of the van der Waals-type approach over the Walecka approach. In the following, we will review this aspect to arrive at the modified equation of state (EoS) of such a nonideal hadron resonance gas (NIHRG) system.

2. The Statistical Approach

In this section, we will attempt to provide an overview of the van der Waals-type EoS for interacting NIHRG which is done by employing the grand canonical ensemble (GCE) formulation with both attractive as well as repulsive interactions taken into account.

The short-range repulsive hard-core interaction exists between the pairs of baryons and also among the pairs of antibaryons, while the antibaryon-baryon pair interactions are dominated by annihilation reaction process inside the evolving hot fireball. These are the limitations of the current model and leave the scope for further improvement in the future [52]. The attraction is therefore assumed to exist between the pairs of two baryons and pairs of two antibaryons. At fixed T and μ, the presence of the parameter $b > 0$, which describes the repulsion between particles, leads to a suppression of particle number density $n(T, \mu)$ whereas the attractive interactions described by $a > 0$ lead to its enhancement [11, 12, 52]. Hence, the attractive interaction will be there even in a baryon-rich system at large chemical potential.

The ideal (i.e., interaction free) grand canonical partition function is given by

$$\mathscr{Z}(T, \mu, V) = \sum_{N=0}^{\infty} e^{\mu N/T} \, \mathscr{Z}(T, N, V). \qquad (1)$$

Here, $\mathscr{Z}(T, N, V)$ represents the canonical partition function for N number of particles. T and V are the temperature and total physical volume of the system, respectively. The phenomenological grand partition function with both the attractive and repulsive interactions taken into account can be written as

$$\mathscr{Z}^{int}(T, \mu, V) = \sum_{N=0}^{\infty} e^{\mu N/T} \mathscr{Z}(T, N, V - bN) e^{-\bar{U}/T}. \qquad (2)$$

Here, N is the number of particles in the system with both attractive and repulsive interactions present (i.e., $N = N^{int}$).

Here, bN represents the excluded volume of baryons (antibaryons) arising due to hard-core repulsive interaction [29, 33–35]. The attractive interaction is taken into account in the form of an average interaction energy through the introduction of the factor $e^{-\bar{U}/T}$ in the grand partition function, where $\bar{U}$ represents the average attractive interaction energy assuming a uniform particle density, $n = N/V$. The mean attractive interaction energy can be written as $\bar{U} = (1/2)\sum_{i,j} V_{att}(\vec{r}_i - \vec{r}_j)$, where $V_{att}(\vec{r}_i - \vec{r}_j)$ represents the average attractive interaction energy of any two particle pairs, which depends on their relative coordinates, $\vec{r} = \vec{r}_i - \vec{r}_j$. Contribution of three or more particle interactions is ignored because such collisions would be rare. Thus, in general, it is sufficient to consider only one pair of particles [41]. Under the assumption of a uniform particle density $n = N/V$, the total interaction energy can be obtained by summing over all the particle pairs. Therefore (for large n), we can write

$$\bar{U} = \frac{1}{2} \int d^3\vec{r}_1 d^3\vec{r}_2 n\left(\vec{r}_1\right) n\left(\vec{r}_2\right) V_{att}\left(\vec{r}_2 - \vec{r}_1\right), \quad (3)$$

which finally yields $\bar{U} = n^2 V u/2$. The quantity $u = \int d^3 \vec{r} V_{att}(\vec{r})$. By defining $a = \int 2\pi r^2 dr V_{att}(\vec{r})$, where "$a$" represents the effective attractive parameter, we can write $u = 2a$. Using equation (3), we finally get $\bar{U} = n^2 V a$.

We can therefore rewrite

$$\mathscr{Z}^{int}(T, \mu, V) = \sum_{N=0}^{\infty} e^{\mu N/T} \mathscr{Z}(T, N, V - bN) e^{-n^2 V a/T}, \quad (4)$$

where $\mathscr{Z}(T, N, V - bN)$ is the canonical partition function taking into account the excluded volume effect arising due to hard-core hadronic repulsion. The pressure function is obtained [29] by identifying the extreme right-hand singularity of the Laplace transform of $\widehat{\mathscr{Z}}^{int}$ in equation (4):

$$\widehat{\mathscr{Z}}^{int}(T, \mu, \zeta) = \int e^{-\zeta V} \mathscr{Z}^{int}(T, \mu, V) dV. \quad (5)$$

The ζ is the parameter of the Laplace transformation. One can rewrite for uniform particle number density:

$$\widehat{\mathscr{Z}}^{int}(T, \mu, \zeta) = \int e^{-\zeta V} \mathscr{Z}^{excl}(T, \mu, V) e^{-n^2 V a/T} dV, \quad (6)$$

where $\mathscr{Z}^{excl}(T, \mu, V) = \sum_{N=0}^{\infty} e^{\mu N/T} \mathscr{Z}(T, N, V - bN)$ is the grand canonical partition function with excluded volume effect taken into account.

The extreme right-hand singularity of the Laplace transformation in equation (6) can be located by rewriting the integrand in equation (6) to get

$$\widehat{\mathscr{Z}}^{int}(T, \mu, \zeta) = \int e^{-V\left(\zeta - \left(\ln \mathscr{Z}^{excl}(T,\mu,V)/V\right) + n^2 a/T\right)} dV. \quad (7)$$

The finiteness of the integral in equation (7) requires

that in the limit $V \longrightarrow \infty$, the extreme right-hand singularity must satisfy

$$\zeta = \frac{1}{T} \lim_{V \to \infty} \left[\frac{T \ln \mathscr{Z}^{excl}(T, \mu, V)}{V} - n^2 a \right]. \quad (8)$$

Defining $p^{excl}(T, \mu, V) = \lim_{V \to \infty} T\{\{\ln Z^{excl}(T, \mu, V)\}/V\}$ and $\zeta T = p^{int}$.

We can then finally write the pressure of the system incorporating the attractive as well as repulsive interaction:

$$p^{int}(T, \mu, V) = p^{excl}(T, \mu, V) - an^2. \quad (9)$$

It may be noted that here $n = n^{int}(T, \mu)$. By taking into account the effect of repulsive interaction, leading to an excluded volume type effect, we can write [29, 35] by considering the available volume in the system:

$$p^{excl}(T, \mu, V) = \frac{nT}{1 - bn}. \quad (10)$$

This gives

$$p^{int}(T, \mu, V) = \frac{nT}{1 - bn} - an^2. \quad (11)$$

The particle number density can then be obtained in a thermodynamically consistent way by using $n = \partial p^{int}/\partial \mu|_T$. This finally yields a relation for the chemical potential:

$$\mu = T \ln \left(\frac{n}{1 - bn} \right) + \frac{T}{1 - bn} - 2an + C. \quad (12)$$

With $C = \mu - T \ln (n^{id}) - T$.

Writing the point-like particle number density $n^{id} = e^{\mu/T}\phi$, we get

$$C = T \ln \left(\frac{n^{id}}{\phi} \right) - T \ln \left(n^{id} \right) - T. \quad (13)$$

Thus, we get

$$\mu = T \ln \left\{ \frac{n}{(1 - bn)\phi} \right\} + \frac{nTb}{1 - bn} - 2an. \quad (14)$$

Defining $\mu^* = T \ln \{n/((1 - bn)\phi)\}$ and writing ϕ in terms of μ^*, i.e., $\phi = n^{id}(T, \mu^*)e^{-\mu^*/T}$ and using this in equation (14), we will get an expression for the "effective" chemical potential, i.e., μ^* and the particle number density n (i.e., n^{int}) as

$$\mu^* = \mu - \frac{nbT}{1 - bn} + 2an, \quad (15)$$

$$n = (1 - bn)n^{id}(T, \mu^*). \quad (16)$$

This finally yields particle number density in the NIHRG model as

$$n(\mu, T) = \frac{n^{id}(T, \mu^*)}{1 + bn^{id}(T, \mu^*)}. \tag{17}$$

Equation (17) is the number density for single component of hadronic matter. For multicomponent baryonic matter, we can generalize the above equation to get

$$n_j\left(\mu_j, T\right) = \frac{n_j^{id}\left(T, \mu_j^*\right)}{1 + \sum_i b_i n_i^{id}\left(T, \mu_j^*\right)}. \tag{18}$$

Equation (18) represents the modified number density of the jth baryonic specie for a multicomponent NIHRG, using the van der Waals-type equation of state (EoS). The excluded volume arising due to the jth baryonic specie, considering it a hard sphere, is $(b_j = (16/3)\pi r_j^3)$, where r_j represents the hard-core radius of the jth baryonic specie. The summation over the index i in the denominator also includes j and is over all the baryonic degrees of freedom, as the hard-core repulsion exists between baryon-baryon pairs or antibaryon-antibaryon pairs. The effect of the attractive and the repulsive hard-core interaction appears in the equation of state of the system through the "effective" baryon chemical potential (μ^*) in equation (15).

The application of equation (15) to the antibaryonic sector requires that the "effective" chemical potential for antibaryon (i.e., $\overline{\mu^*}$) be written as

$$\overline{\mu^*} = \overline{\mu} - \frac{\overline{n}bT}{1 - b\overline{n}} + 2a\overline{n} \text{ with } \overline{\mu} = -\mu, \tag{19}$$

where the quantities with bar indicate their values for the antibaryons. For the antibaryonic sector in the multicomponent NIHRG, we will get

$$n_{\overline{j}} = \frac{n_j^{id}\left(T, \overline{\mu_j^*}\right)}{1 + \sum_i b_{\overline{i}} n_i^{id}\left(T, \overline{\mu_j^*}\right)}. \tag{20}$$

For a baryon free matter, $\overline{\mu_j} = -\mu_j = 0$. This also gives $\overline{\mu_j^*} = \mu_j^*$, thus providing $n_j = n_{\overline{j}}$ at any given temperature T, which is mandatory to maintain the baryon-antibaryon symmetry in the system when $\mu_j = 0$. In equation (20), the summation over the index i in the denominator is over all the antibaryonic degrees of freedom. In the following, we present results of our numerical calculations and discussion.

3. Results and Discussion

Making use of the above results, we have calculated relative particle yields which may be compared with the experimental data at various energies such as SPS and RHIC in order to determine the final stage freeze-out conditions in the fireballs formed in these experiments.

With this aim, we have applied the above formulation for a system of hot and dense hadronic matter consisting of several hadronic species. The repulsive forces are assumed to exist between pairs of two baryons (fermions) and pairs of two antibaryons (antifermions), while it is purely attractive between baryon-antibaryon pairs. This is consistent with earlier approaches [33–35]. We have calculated various particle ratios and studied their variations with changes in temperature (T) and baryon chemical potential (μ_B) of the system. This is essentially done to see the effect of the van der Waals-type interaction on the number densities of different hadronic species as well as their relative abundances for the nonideal multicomponent hadron resonance gas (NIHRG) and compare the above results with those which are obtained for the point-like ideal hadron resonance gas (IHRG). The results are found to depend on the system's temperature and chemical potential.

At collision energy ranges of the experiments at RHIC, SPS, and also in the upcoming CBM and MPD-NICA [53] experiments, the nuclear stopping effect is expected to be fairly high leading to a baryon-rich fireball. The baryon-rich fireballs are expected to maintain large chemical potentials which will vary with the degree of stopping in the given experiment. Variation in system's temperature will also be observed depending on the collision scenario, including system size [27, 28].

In many earlier works employing different model approaches, the values of the attractive parameter a have been used in the range 329-1250 MeV-fm^3. The repulsive parameter $b = ((16/3)\pi r_0^3)$ was fixed by choosing a suitable value of the hadronic hard-core radius r_0. We have used a constant value of the attractive parameter $a = 329$ Mev-fm^3 and $r_0 = 0.59$ fm. These values of the parameters in the van der Waals-type EoS are fixed by the ground state properties of cold ($T \approx 0$) nuclear matter [11, 12, 51, 52, 54–57]. In another approach, $r_0 = 0.7$ fm has also been used in a meson mean-field-type model EoS to determine the ground state nuclear matter incompressibility [29].

While attempting to describe the properties of the hadronic matter formed in the ultrarelativistic nucleus-nucleus collisions, we are essentially dealing with a system of strongly interacting particles; hence, the quantities such as baryon number and strangeness are conserved within the system. The weakly decaying particles such as lambda, sigma, and cascade also contribute to the observed lighter hadron multiplicities. However, at the strong interaction time scale, these decays take place long after the freeze-out of the strongly interacting hadronic matter has taken place. Moreover, as already discussed in the previous section, the total number of particles within the system before its final break-up is not fixed due to continuous creation, annihilation, and other reaction processes. Thus, the conservation of mean baryon number and the mean net strangeness content of the system is achieved within the framework of the grand canonical ensemble. This is done by introducing the baryon and strange chemical potentials, μ_B and μ_s, respectively. Considering three quark flavours, we have in our calculation defined the chemical potentials of a given j^{th} hadron as [19, 20, 37, 58–64]

$$\mu_i = (q_i - \overline{q}_i) \mu_q + (s_i - \overline{s}_i) \mu_s = N_q \mu_q + N_s \mu_s, \tag{21}$$

where N_q and N_s are the number of valence light (u, d) and strange (s) quarks, respectively, in a given j^{th} type hadronic specie with $\mu_q = \mu_B/3$.

In the following, we present our results for the dependence of the "effective" baryon chemical potential, μ_B^*, and various "relative" hadronic yields. We discuss their dependence on the thermal parameters of the system, i.e., T and μ_B. For this purpose, we have included in our system hadronic resonances up to the omega mass (1672 MeV) and used their known weak decay channels to calculate their contributions to the lower mass hadronic multiplicities after the thermochemical freeze-out of the system has occurred.

We have determined the effective baryon chemical potential μ_B^* by solving transcedental equations (15) and (18). In Figure 1, we have shown the variation of μ_B^* with temperature for a baryon-rich system by choosing $\mu_B = 300$ MeV and 500 MeV. We find that as the temperature increases beyond 80 MeV, the μ_B^* shows a very slightly increase, but beyond $T \sim 120$–130 MeV, it starts decreasing rapidly.

This effect is further highlighted in Figure 2 where we have shown the dependence of the "relative" effective baryon chemical potential, i.e., μ_B^*/μ_B with T for $\mu_B = 300$ MeV and 500 MeV.

In the ultrarelativistic nucleus-nucleus collisions, the antiproton-to-proton ratio ($\bar{p}/p$) is considered an important indicator of the degree of nuclear stopping. This also allows us to learn how baryon numbers initially carried by the nucleons only, before the nuclear collision, are distributed in the final state [65–71]. With this aim, we have in Figure 3 the dependence of antiproton-to-proton ratio ($\bar{p}/p$) on temperature at two fixed values of baryon chemical potential, $\mu_B = 300$ MeV and 500 MeV. For each case (viz., the point-like IHRG and NIHRG cases), we have considered two situations in our calculations, i.e., when the weak decay contributions of heavier resonances after the freeze-out are included and when they are ignored. The $\bar{p}/p$ ratio increases with increasing temperature for all cases. This essentially happens since the numbers of *directly* produced $\bar{p}$ and those produced by the *decaying* antibaryons after the freeze-out increase due to their enhanced thermal production, which would be otherwise suppressed due to high chemical potential in a baryon-rich system. The decay contributions are seen to further increase this ratio compared to the situation when they are not taken into account. In the case of the NIHRG, the $\bar{p}/p$ ratio is seen to increase appreciably. Thus, the interactions incorporated in the NIHRG system may play an important role in determining the actual freeze-out conditions in a hot baryon-rich system, i.e., at sufficiently large values of μ_B and T.

The midrapidity $\bar{p}/p$ ratio in central Pb+Pb collisions at 40 A GeV in CERN-SPS experiments is ≈ 0.0078 [72, 73]. In the above results, if we chose $\mu_B = 500$ MeV and $T \sim 160$ MeV, we obtain a good description of this ratio if we use the equation of state of NIHRG. Similarly, the experimental midrapidity $\bar{p}/p$ ratio at 80 A GeV is ≈ 0.028 [73] and can be obtained for $\mu_B = 300$ MeV and $T \sim 155$ MeV. In all thermal models, the value of the baryon chemical potential μ_B essentially indicates the excess of baryons over antibaryons. We
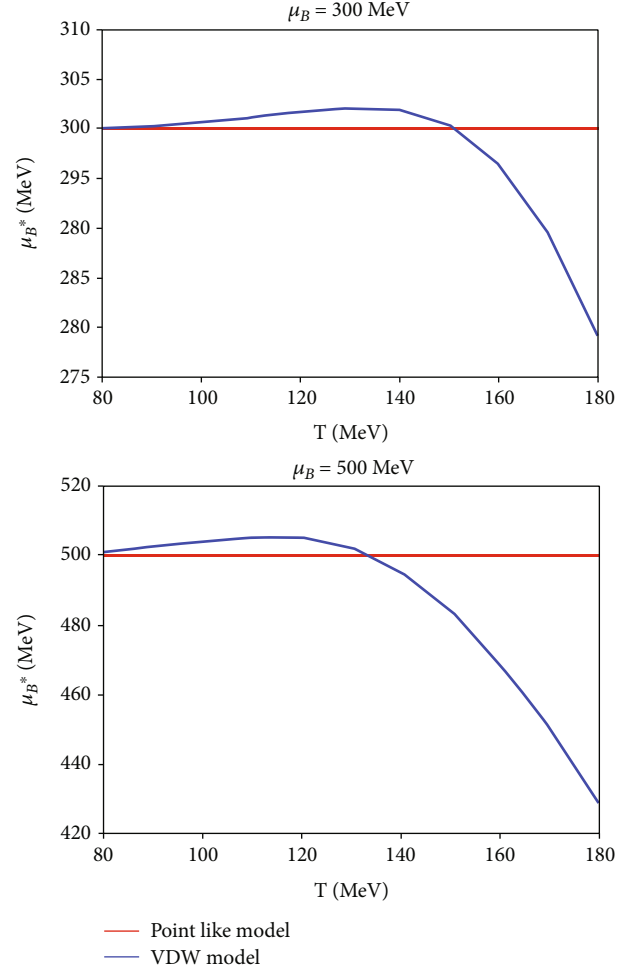

FIGURE 1: Variation of "effective" baryon chemical potential with temperature, T, in a baryon-rich system for two fixed values of baryon chemical potential, $\mu_B = 300$ MeV and 500 MeV.

therefore expect the system to maintain a larger chemical potential at 40 A GeV as compared to 80 A GeV due to relatively lesser thermal production of antibaryons (including antihyperons) hence leading to a relatively large excess of baryons over antibaryons at 40 A GeV as compared to 80 A GeV.

With nonconsideration of the resonance decay and more importantly the interaction in the HRG, one would need a significantly large value of temperature at this value of chemical potential to reproduce the $\bar{p}/p$ ratio value which may seem somewhat unphysical. However, one may still get a reasonable value of this ratio in IHRG case at a lower value of T by choosing a smaller value of μ_B.

As indicated at these energies since the nuclear stopping is effective, hence the system formed in such collisions is expected to be baryon rich, i.e., with high net baryon density, and therefore will maintain sufficiently large chemical potential [25, 65, 74–81]. Hence, the determination of the values of chemical potential and temperature of the system at freeze-out can help us understand the degree of nuclear stopping. As one moves up from SPS to RHIC energy,
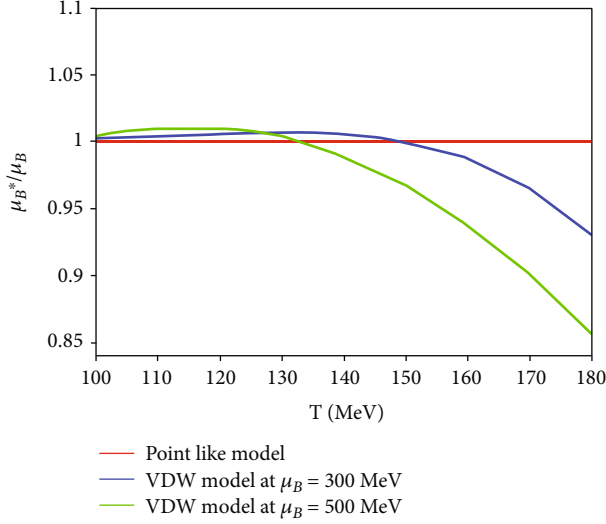
FIGURE 2: Variation of "relative" effective baryon chemical potential with temperature, T, in a baryon-rich system for two fixed values of baryon chemical potential, $\mu_B = 300$ MeV and 500 MeV.

approximately the same temperature but a significantly smaller baryonic chemical potential is observed in the central rapidity region [25, 65, 82, 83]. Theoretical extraction of these values will depend on the choice of the statistical model used for analyzing the experimental data.

Experiments have shown enhancement in the overall strangeness production in the nuclear collisions at ultrarelativistic energies relative to the nonstrange hadrons. Therefore, experimental measurement of the strange hyperons created in nuclear collisions is also an important tool to study the properties of the hot and dense systems typically produced in nuclear collisions at ultrarelativistic energies. Unlike hadron-hadron collisions, we expect that in the most central ultrarelativistic nuclear collisions, the *participating* quarks will scatter many times before joining in an asymptotic hadronic state at the stage of hadronization. Application of the well-established methods of statistical physics can provide a simplified approach to theoretically predict the strangeness abundance [83]. Such attempts have been made earlier also to describe strangeness production in ultrarelativistic nucleus-nucleus collisions in terms of an equilibrated gas of hadronic resonances [60–64].

In the statistical thermal approach, the abundance of strange particles in the system is affected not only by the values of μ_B and T but also by the value of the strange chemical potential, μ_s, which, as already stated previously, is fixed by the strangeness conservation criteria for the given values of μ_B and T.

In Figure 4, we have plotted the variation of "effective" *strange chemical potential* (μ_s^*) with temperature T for $\mu_B = 300$ MeV and 500 MeV. The strange baryon chemical potential value obtained using the van der Waals-type interaction in NIHRG model is compared with the point-like hadron case (i.e., IHRG). We notice that after initial decrease, the "effective" strange chemical potential (μ_s^*) gets enhanced in
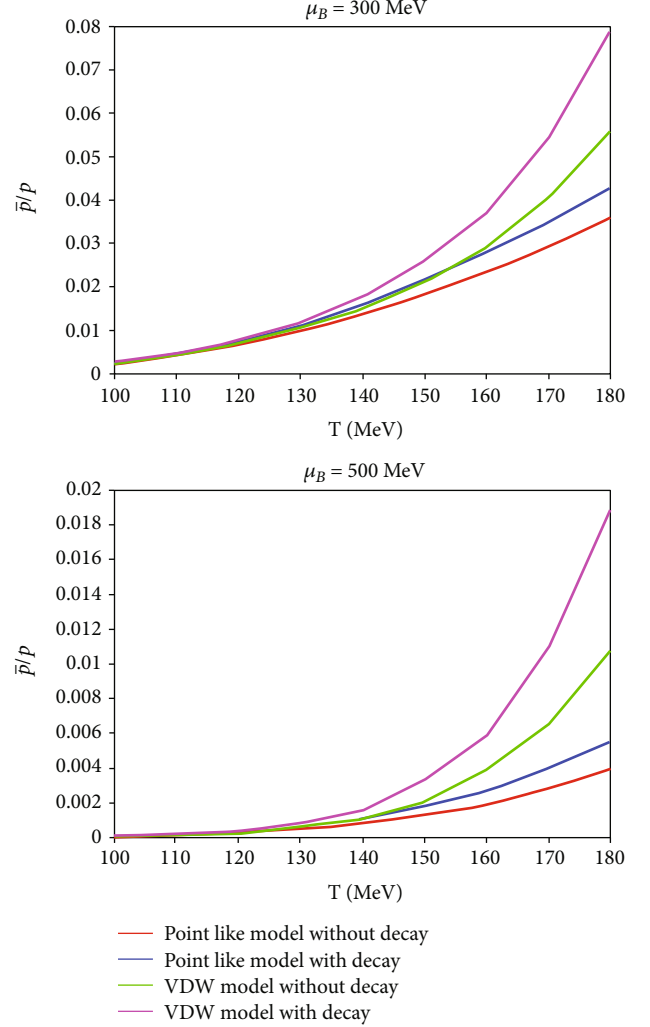

FIGURE 3: Dependence of the $\bar{p}/p$ ratio on temperature for $\mu_B = 300$ MeV and 500 MeV.

presence of the van der Waals (VDW) type interactions in the HRG as compared in point-like hadron case, especially at higher temperatures and chemical potentials.

The antistrange-to-strange hyperon ratios using NIHRG as well as IHRG equation of states have been calculated. This will also enable us to understand that to what extent the "effective" baryon as well as the corresponding "effective" strange chemical potentials, i.e., μ_B^* and μ_s^*, can affect these ratios.

With this purpose, we have first calculated the singly antistrange-to-strange particle ratio, viz., $(\bar{\Lambda}/\Lambda)$.

The curves in Figure 5 show that inclusion of the resonance decay contribution can play a very important role here. A significant increase in the $(\bar{\Lambda}/\Lambda)$ ratio is observed with decay contributions taken into account for both cases, i.e., IHRG and NIHRG. For the NIHRG case, the ratio shows significant increase for temperatures above 160 MeV. The available experimental data at midrapidity from NA49 collaboration [84] gives the values of this ratio at 40 A GeV and 80 A GeV in CERN-SPS experiments as ~0.027 and
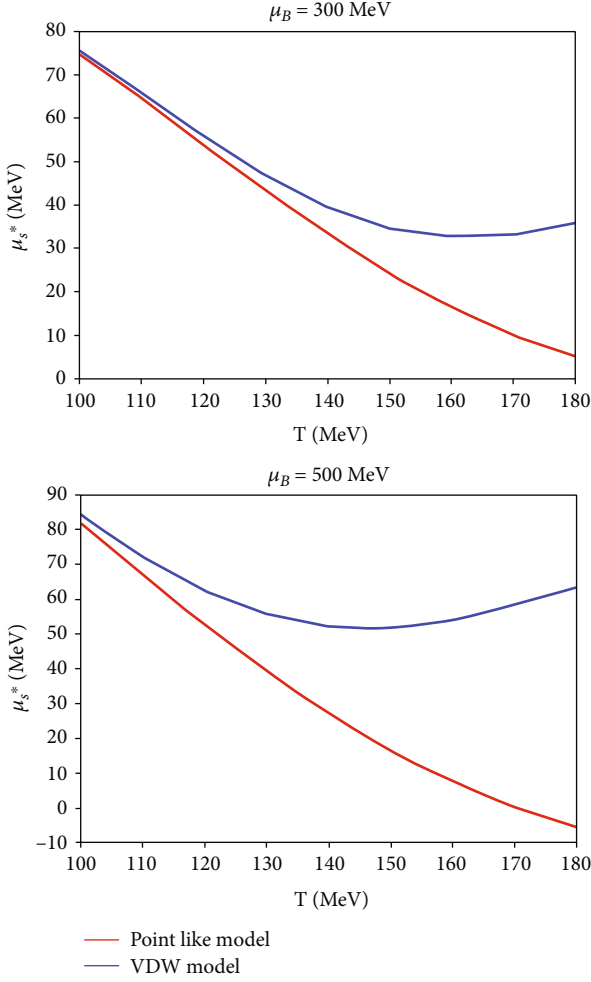
FIGURE 4: Variation of "effective" strange chemical potential (μ_s^*) with temperature at fixed baryon chemical potentials $\mu_B = 300$ MeV and 500 MeV.

FIGURE 5: Dependence of the ratio ($\bar{\Lambda}/\Lambda$) on temperature at fixed baryon chemical potential $\mu_B = 300$ MeV and 500 MeV.

0.078, respectively. These can be well reproduced by using NIHRG model using $\mu_B = 500$ MeV and 300 MeV, respectively, for temperatures close to ~155-160 MeV.

Measurement of "relative" strange hadron yield provides a better understanding of the strangeness production mechanism in nucleus-nucleus collisions. Using the IHRG as well as the NIHRG models, we have calculated Λ/p ratio and Figure 6 shows its dependence on the temperature of the system for $\mu_B = 300$ MeV and 500 MeV.

It is interesting to see that using the EoS of IHRG, the inclusion of resonance decay contribution leads to an enhancement of Λ/p ratio while the behaviour of the system using EoS of the NIHRG the opposite is observed. The values of this ratio at 40 A GeV and 80 A GeV can be obtained from CERN-SPS experiment [73, 84] results, which turn out to be about 0.35 and 0.42, respectively. In the present calculation, these can be reproduced by the NIHRG model results quite well for $\mu_B \approx 500$ MeV and 300 MeV, respectively, for temperatures close to ~165 MeV taking into account the decay contributions. The IHRG model with con-
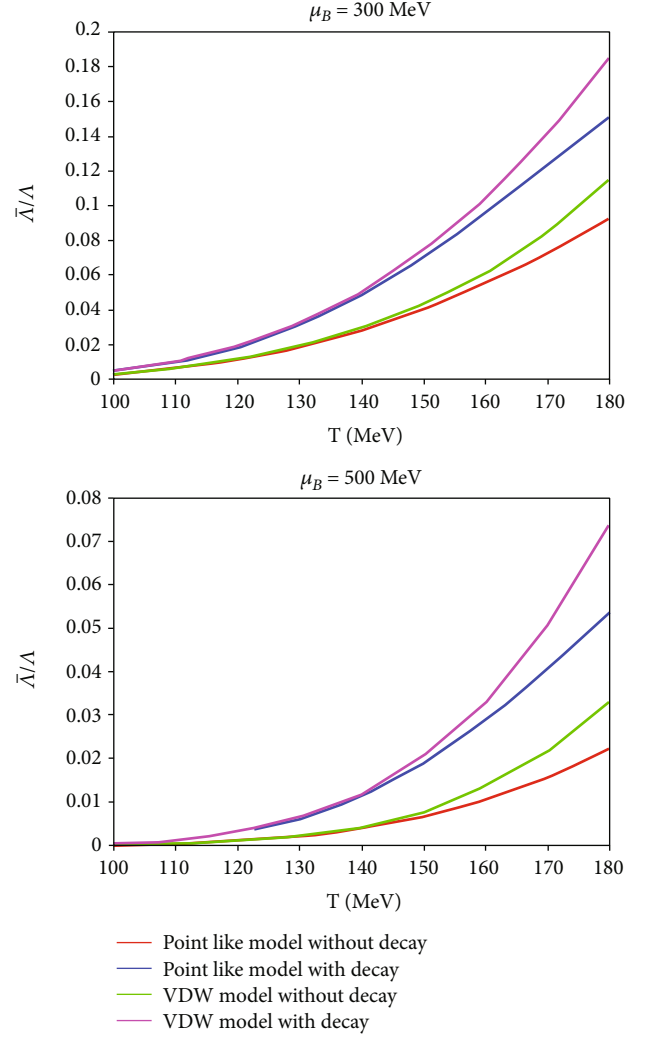
tribution of the decay products taken into account is seen to over predict this ratio and can therefore reproduce the experimental values only at much lower temperatures.

Figure 7 shows the variation of the doubly (anti)strange particle ratios, i.e., anticascade to cascade ($\bar{\Xi}/\Xi$). In this case, we notice that when we use the van der Waals (VDW) type EoS, there is a slight decrease in ($\bar{\Xi}/\Xi$) ratio compared to the point-like hadron case at high temperatures, especially for a baryon-rich system. The available experimental data at 40 A GeV in Pb+Pb collision gives this ratio ~0.07 [85] which can be well described around T ~155 MeV in case of NIHRG and ~145 MeV for IHRG for $\mu_B \approx 500$ MeV. The same ratio at 80 A GeV is found to be ~0.17 and can be described by both models around T ~154 MeV for $\mu_B \approx 300$ MeV [84].

In almost all the above cases, we find that the NIHRG EoS can consistently reproduce the experimental particle ratios for the two CERN-SPS energies in the temperature range of 155–165 MeV which appears quite reasonable.

Another interesting particle ratio, viz., (K^-/K^+), has been shown in Figure 8. We find that for both values of
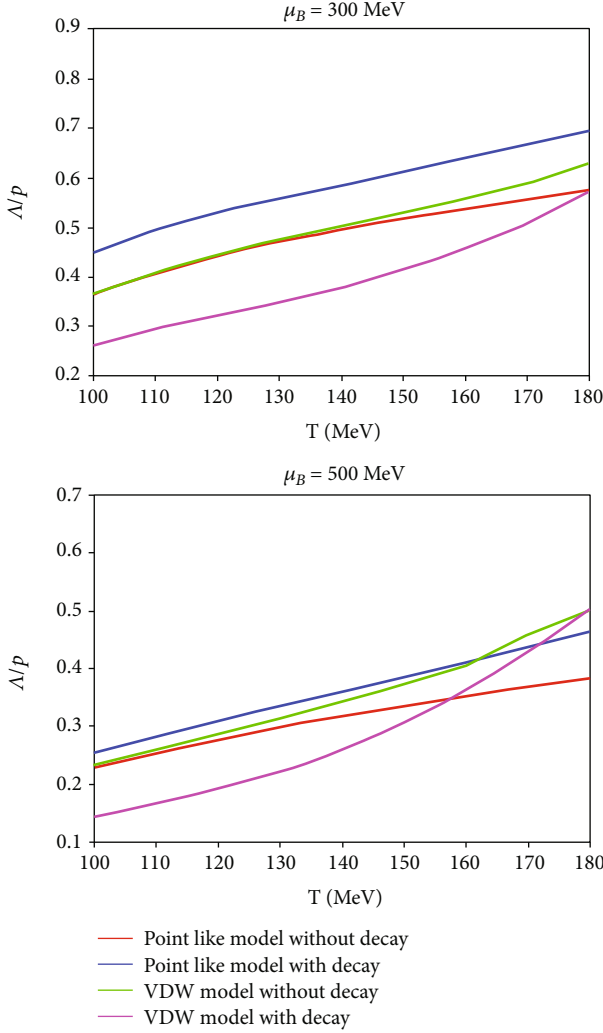
FIGURE 6: Dependence of the ratio (Λ/p) on freeze-out temperature at fixed baryon chemical potential $\mu_B = 300$ MeV and 500 MeV.

FIGURE 7: Ratio of doubly (anti)strange particles, ($\bar{\Xi}/\Xi$) dependence on temperature for baryon-rich systems.

chemical potential, the ratio for the two cases, i.e., IHRG and NIHRG, initially decreases. But for the case of NIHRG, it shows a rising trend after certain value of temperature. This behaviour of NIHRG with VDW type interaction is in contrast with that of the IHRG. Further, K^-/K^+ ratio is seen to be suppressed when heavier hadronic resonance decay contributions are taken into account, especially at smaller temperatures. But at higher temperatures, the NIHRG result with decay contributions taken into account leads all the other three cases.

The available integrated data from NA49 at 80 A GeV from the Pb+Pb collision [86] gives ≈0.37, which is seen reasonably close to the IHRG curve for $\mu_B = 300$ MeV when T ~145 MeV provided resonance decay contributions are taken into account. Without these contributions, the IHRG result highly over predicts the experimental data at this temperature. At this value of μ_B, the NIHRG result with resonance contributions taken into account is also seen to somewhat over predict this value. In NIHRG case, however one can obtain this value of (K^-/K^+) ratio at nearly the same
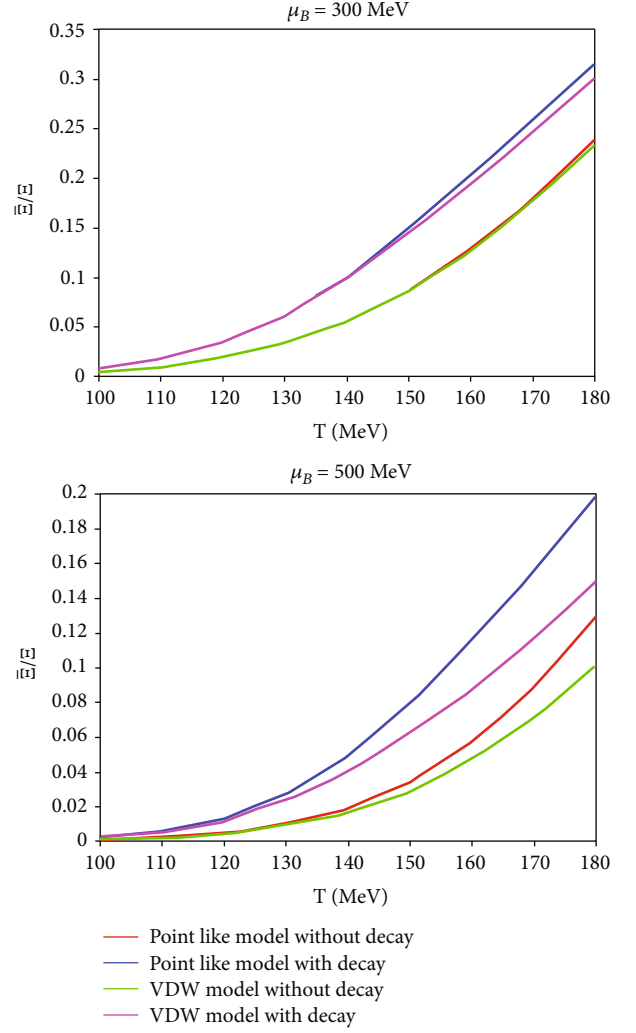
temperatures (~155–165 MeV) used for the other particle ratios above if we use a somewhat larger value of μ_B ~350-375 MeV.

In reference [87], the authors have employed the statistical thermal freeze-out model to obtained particle ratios considering point-like hadrons. Using their approach, they have obtained $\mu_B ≈380$ MeV and $T ≈147$ MeV for Pb+Pb collisions at 40 A GeV, and at 80 A GeV, their values are $\mu_B ≈297$ MeV and $T ≈153$ MeV. Thus, at 40 A GeV, the value of the freeze-out chemical potential in our case (μ_B ≈500 MeV) is higher while it is nearly same (≈300 MeV) at 80 A GeV. The freeze-out temperature values in our case are found to be slightly higher (155–165 MeV). Similarly, in reference [82], the authors have also analyzed the experimental particle ratio data and extracted the chemical and kinetic freeze-out parameters. They have obtained $\mu_B ≈400$ MeV and $T ≈140$ MeV for collisions at 40 A GeV, while at 80 A GeV, they have obtained μ_B ≈300 MeV and $T ≈144$ MeV. We find that at 40 A GeV, our analysis again gives a somewhat higher value of μ_B
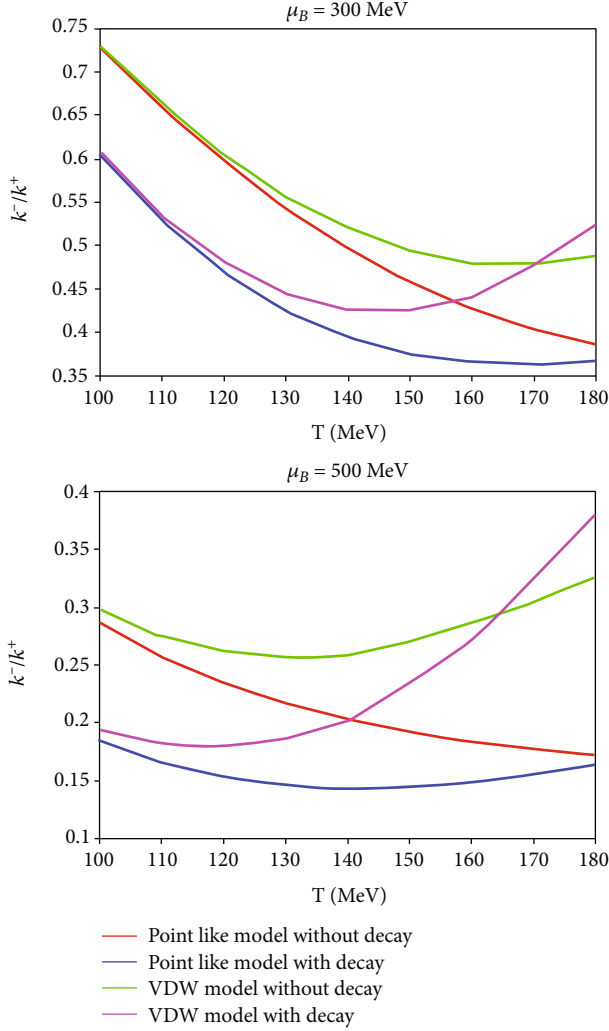
FIGURE 8: The (K^-/K^+) ratio with temperature for baryon-rich system using $\mu_B = 300$ MeV and 500 MeV.

(≈ 500 MeV) and temperature T (≈ 155 MeV). At 80 A GeV, the extracted values of chemical potential in all cases, including ours, are almost the same, i.e., ≈ 300 MeV, while the freeze-out temperature in our case is in the range of 155–165 MeV, which is higher than those obtained in the two cases mentioned above.

The range of the freeze-out temperature obtained in all such thermal models using experimental particle ratio data is somewhat larger than the typical critical values of the temperature required for a first-order phase transition between the QGP and HRG phases. Some thermodynamic model-based calculations have also suggested that there may be a critical end point (CEP) in QCD matter where the first-order phase transition ends and thereafter the transition becomes a crossover [88, 89]. The parameters extracted from the experimental data lead us to estimate properties of the hot hadronic matter at freeze-out. Such predictions of the freeze-out temperature and chemical potential may have an important effect on the existence and location of a putative CEP in the first-order QCD phase diagram [90]. There is still theoretical debate as to whether such a critical point

exists at all. Based on the lattice gauge theory calculations, one expects that a crossover region may occur at T_c $(\mu_B = 0) = 154 \pm 9$ MeV and $\varepsilon_c = 0.18 - 0.5$ GeV/fm^3 [91, 92]. Some results even indicate that the location of a critical end point might be disfavoured for $\mu_B/T \leq 2$ and T/T_C $(\mu_B = 0) > 0.9$ [92, 93]. QCD-based models predict a first-order phase transition and the existence of an end point or critical point at high μ_B as well. However, the locations of the phase boundary and the CEP in this framework depend on model assumptions [23, 94–96]. It is suggested that the LQCD calculations however cannot be used to directly determine the position of this CEP. The CEP has not yet been found for $\mu_B/T \leq 2$ and $145 \leq T \leq 155$ MeV [97–99]. The results of the search for the CEP and the first-order phase boundary have narrowed the region of interest to collision energies below $\sqrt{s_{NN}} = 20$ GeV. But the experimental evidence of a CEP and first-order phase transition at higher μ_B remains to be confirmed experimentally [100].

In an experimental measurement, the net-charge fluctuations in pp and light nuclei (Ar-Sc) collisions have been investigated by NA61/SHINE for $\sqrt{s_{NN}} = 6$-12 GeV as it is suggested that a crossover beyond CEP would result in large particle fluctuations. It is concluded that there is no evidence for a critical end point from these data [91]. The abovementioned energy range approximately covers the SPS energy range of 40 A GeV to 80 A GeV. In some work, it has been even reported that QCD phase transition temperature may lie in the vicinity 170-180 MeV for $\mu_B \approx 0$ [101].

In the light of the above and the freeze-out temperature values obtained in our as well as other analyses, which are in generally the range of 155-165 MeV, it appears that if the critical end point exists at all, then it might be located above this temperature range for a reasonably baryon-rich system $(\mu_B \approx 200$–300 MeV) [91]. From the analysis, it further appears that the hadrons freeze out shortly after the phase transition [30, 100]. The kinetic freeze-out temperatures reported in the analysis of the experimental p_T spectra in various works are also in the vicinity of the temperature range mentioned above. Cleymans et al. have reported the values of the freeze-out parameters determined through statistical thermal models using particle yields by various groups [102]. It may thus indicate the existence of higher phase transition or crossover temperature values in the experiments.

4. Summary and Conclusion

Within the framework of a statistical thermal model, we have used a grand canonical ensemble formulation for a multicomponent nonideal hadron resonance gas model. We have considered the attractive as well as repulsive interactions among the constituent baryons (antibaryons). The particle number densities are obtained in a thermodynamically consistent manner. Using the present formulation, we have calculated several particle ratios like $\bar{p}/p$, $\bar{\Lambda}/\Lambda$, Λ/p, $\bar{\Xi}/\Xi$, and K^-/K^+. The dependence of these relative particle yields, the "effective" baryon chemical potential (μ_B^*), and the "effective" strange chemical potential (μ_s^*) on T and μ_B has been studied. We find that the particle ratios get

modified particularly at higher values of T and μ_B by using the van der Waals-type EoS, i.e., considering the existence of a nonideal hadronic resonance gas (NIHRG) at the hadronic fireball freeze-out which is assumed to be in a state of reasonably high degree of thermochemical equilibrium. The application of the NIHRG equation of state shows that these interactions can play important role in describing the relative particle yields especially for a hot baryon-rich system. We find that by considering the formation of a NIHRG system in the ultrarelativistic nucleus-nucleus collisions we can quite reasonably predict several experimental particle ratios obtained in the CERN SPS at 80 A and 40 A GeV within a temperature range of 155–165 MeV and choosing μ_B values 300 MeV and 500 MeV for the two cases, respectively.

Elaborate analyses of the hadronic yields for a baryon-rich system can be carried out further when data from the upcoming compressed baryonic matter from the FAIR experiments will become available. This paper is available on the arXiv website [103].

Data Availability

The data supporting for this work is at RHIC and SPS websites.

Disclosure

This updated version of the manuscript is available on the arXiv website bearing ID arXiv: 1912.08134 [hep-ph].

Conflicts of Interest

The authors declare that they have no conflict of interest.

Acknowledgments

References

[1] A. Craig, "Strangeness production at the AGS," *Journal de Physique*, vol. 23, no. 12, pp. 1803–1816, 1997.

[2] P. Seyboth, "Strange particle production in ultrarelativistic heavy ion collisions at the CERN SPS," *Journal de Physique*, vol. 23, no. 12, pp. 1787–1801, 1997.

[3] Christian Bormann (NA49 Collaboration), "Kaon-, Λ^- and $\bar{\Lambda}$-production in Pb+Pb - collisions at 158 GeV per nucleon," *Journal of Physics G: Nuclear and Particle Physics*, vol. 23, article 1817, 1997.

[4] STAR Collaboration, "Strange and multistrange particle production in Au + Au collisions at $\sqrt{S_{NN}} = 62.4$ GeV," *Physical Review C*, vol. 83, article 024901, 2011.

[5] ALICE Collaboration, "Centrality dependence of charged particle production at large transverse momentum in Pb–Pb collisions at $\sqrt{S_{NN}} = 2.76$ TeV," *Physics Letters B*, vol. 720, pp. 52–62, 2013.

[6] F.-H. Liu, S. Fakhraddin, and B. K. Singh, "Multiparticle production in high energy collisions," *Advances in High Energy Physics*, vol. 2013, Article ID 528352, 2 pages, 2013.

[7] J. Rafelski, *Final Research Report 2004 – 2015*, University of Arizona, 2016.

[8] BRAHMS Collaboration, "Rapidity and centrality dependence of particle production for identified hadrons in Cu + Cu collisions at $\sqrt{S_{NN}} = 200$ GeV," *Physical Review C*, vol. 94, article 014907, 2016.

[9] ALICE collaboration, "Enhanced production of multi-strange hadrons in high-multiplicity proton–proton collisions," *Nature Physics*, vol. 13, pp. 535–539, 2017.

[10] P. Foka and M. A. Janik, "An overview of experimental results from ultra-relativistic heavy-ion collisions at the CERN LHC: bulk properties and dynamical evolution," *Reviews in Physics*, vol. 1, pp. 154–171, 2016.

[11] V. Vovchenko, D. V. Anchishkin, and M. I. Gorenstein, "Van der Waals equation of state with Fermi statistics for nuclear matter," *Physical Review C*, vol. 91, article 064314, 2015.

[12] V. Vovchenko, D. V. Anchishkin, and M. I. Gorenstein, "Particle number fluctuations for the van der Waals equation of state," *Journal of Physics A: Mathematical and Theoretical*, vol. 48, article 305001, 2015.

[13] J. Cleymans and H. Satz, "Thermal hadron production in high energy heavy ion collisions," *Physica C*, vol. 57, no. 1, pp. 135–147, 1993.

[14] F. Becattini, J. Cleymans, A. Keranen, E. Suhonen, and K. Redlich, "Features of particle multiplicities and strangeness production in central heavy ion collisions between 1.7A and 158 AGeV/c," *Physical Review C*, vol. 64, article 024901, 2001.

[15] P. Braun-Munzinger, D. Magestro, K. Redlich, and J. Stachel, "Hadron production in Au-Au collisions at RHIC," *Physics Letters B*, vol. 518, pp. 41–46, 2001.

[16] J. Rafelski and J. Letessier, "Testing limits of statistical hadronization," 2003, https://arxiv.org/abs/nucl-th/0209084.

[17] A. Andronic, P. Braun-Munzinger, and J. Stachel, "Hadron production in central nucleus–nucleus collisions at chemical freeze-out," *Nuclear Physics A*, vol. 772, p. 167, 2006.

[18] F. Becattini, J. Manninen, and M. Gazdzicki, "Energy and system size dependence of chemical freeze-out in relativistic nuclear collisions," *Physical Review C*, vol. 73, article 044905, 2006.

[19] J. Cleymans, R. V. Gavai, and E. Suhonen, "Quarks and gluons at high temperatures and densities," *Physics Reports*, vol. 130, no. 4, pp. 217–292, 1986.

[20] P. Koch, B. Muller, and J. Rafelski, "Strangeness in relativistic heavy ion collisions," *Physics Reports*, vol. 142, no. 4, pp. 167–262, 1986.

[21] J. E. Alam, E. Sarkisyan-Grinbaum, and S. Bhattacharyya, "Physics of quark gluon plasma: an update and the status report," *Advances in High Energy Physics*, vol. 2014, Article ID 825041, 1 pages, 2014.

[22] J. Rafelski, "Discovery of quark-gluon plasma: strangeness diaries," *The European Physical Journal Special Topics*, vol. 229, no. 1, pp. 1–140, 2020.

[23] M. A. Stephanov, "QCD phase diagram and the critical point," *International Journal of Modern Physics A*, vol. 20, pp. 4387–4392, 2005.

[24] S. Nagamiya, "Heavy-ion collisions toward high-density nuclear matter," *Entropy*, vol. 24, no. 4, p. 482, 2022.

[25] S. Uddin, J. S. Ahmad, W. Bashir, and R. A. Bhat, "A unified approach towards describing rapidity and transverse momentum distributions in a thermal freeze-out model," *Journal of Physics G: Nuclear and Particle Physics*, vol. 39, no. 1, article 015012, 2012.

[26] S. Uddin, I.-u. Bashir, and R. A. Bhat, "Transverse momentum distributions of hadrons produced in Pb-Pb collisions at LHC energy $\sqrt{S_{NN}} = 2.76$ TeV," *Advances in High Energy Physics*, vol. 2015, Article ID 154853, 7 pages, 2015.

[27] S. Uddin, R. A. Bhat, I.-u. Bashir, W. Bashir, and J. S. Ahmad, "Systematic of particle thermal freeze-out in a hadronic fireball at RHIC," *Nuclear Physics A*, vol. 934, p. 121, 2015.

[28] R. A. Bhat, S. Uddin, and I.-u. Bashir, "Unified thermal freeze-out model and its parameters at RHIC," *Nuclear Physics A*, vol. 935, pp. 43–51, 2015.

[29] D. H. Rischke, M. I. Gorenstein, H. Stöcker, and W. Greiner, "Excluded volume effect for the nuclear matter equation of state," *Zeitschrift für Physik C Particles and Fields*, vol. 51, no. 3, pp. 485–489, 1991.

[30] I.-u. Bashir, R. A. Parra, H. Nanda, and S. Uddin, "Energy dependence of particle ratios in high energy nucleus-nucleus collisions: a USTFM approach," *Advances in High Energy Physics*, vol. 2018, Article ID 9285759, 9 pages, 2018.

[31] I.-u. Bashir, R. A. Parra, R. A. Bhat, and S. Uddin, "Particle transverse momentum distributions in p-p collisions at $\sqrt{S_{NN}} = 0.9$ TeV," *Advances in High Energy Physics*, vol. 2019, Article ID 8219567, 7 pages, 2019.

[32] W. Greiner, L. Neise, and H. Stocker, *Thermodynamics and Statistical Mechanics*, Springer-Verlag, New York, Inc., 1995.

[33] S. Uddin and C. P. Singh, "Equation of state of finite-size hadrons: thermodynamical consistency," *Zeitschrift für Physik C Particles and Fields*, vol. 63, pp. 147–150, 1994.

[34] Saeeduddin, "Thermodynamical consistency of the EOS of finite-size hadrons and the quark-hadron phase transition," *Physics Letters B*, vol. 341, p. 361, 1995.

[35] H. Kuono and F. Takagi, "Excluded volume, bag constant and hadron-quark phase transition," *Zeitschrift für Physik C Particles and Fields C*, vol. 42, p. 209, 1989.

[36] T. Endo, T. Maruyama, S. Chiba, and T. Tatsumi, "Finite-size effects on the hadron-quark mixed phase," *AIP Conference Proceedings*, vol. 847, p. 380, 2006.

[37] Saeed-Uddin, "Quark-hadron phase transition and strangeness conservation constraints," *The European Physical Journal C*, vol. 6, no. 2, pp. 355–363, 1999.

[38] T. K. Herbst, M. Mitter, J. M. Pawlowski, B.-J. Schaefer, and R. Stiele, "Thermodynamics of QCD at vanishing density," *Physics Letters B*, vol. 731, pp. 248–256, 2014.

[39] S. Borsanyi, C. H. Zoltan, S. D. Katz, S. Krieg, C. Ratti, and K. K. Szaboo, "Is there still any T*c* mystery in lattice QCD? Results with physical masses in the continuum limit III," *Journal of High Energy Physics*, vol. 1009, p. 73, 2010.

[40] H. Hansen, R. Stiele, and P. Costa, "Quark and Polyakov-loop correlations in effective models at zero and nonvanishing density," *Physical Review D*, vol. 101, article 094001, 2020.

[41] L. D. Landau and E. M. Lifshitz, *Statistical Physics*, Pergamon, Oxford, 1975.

[42] R. A. Parra, S. Uddin, I.-u. Bashir, H. Nanda, W. Bashir, and R. Ahmad, "Study of pion transverse momentum distributions in ultra-relativistic heavy ion collisions: a USTFM approach," *Journal of Experimental and Theoretical Physics*, vol. 129, no. 2, pp. 217–228, 2019.

[43] Y. Hama, T. Kodama, and O. Socolowski Jr., "Topics on hydrodynamic model of nucleus-nucleus collisions," *Journal de Physique*, vol. 35, no. 1, pp. 24–51, 2005.

[44] K. Werner, I. Karpenko, T. Pierog, M. Bleicher, and K. Mikhailov, "Event-by-event simulation of the three-dimensional hydrodynamic evolution from flux tube initial conditions in ultrarelativistic heavy ion collisions," *Physical Review C*, vol. 82, article 044904, 2010.

[45] A. V. Merdeev, L. M. Satarov, and I. N. Mishustin, "Hydrodynamic modeling of the deconfinement phase transition in heavy-ion collisions in the NICA–FAIR energy domain," *Physical Review C*, vol. 84, article 014907, 2011.

[46] J. D. Walecka, "A theory of highly condensed matter," *Annals of Physics*, vol. 83, no. 2, pp. 491–529, 1974.

[47] D. Anchiskin and V. Vovchenko, "Mean-field approach in the multi-component gas of interacting particles applied to relativistic heavy-ion collisions," *Journal of Physics G: Nuclear and Particle Physics*, vol. 42, no. 10, article 105102, 2015.

[48] P. Alba, V. Vovchenko, M. I. Gorenstein, and H. Stoecker, "Flavor-dependent eigenvolume interactions in a hadron resonance gas," *Nuclear Physics A*, vol. 974, pp. 22–34, 2018.

[49] B. D. Serot and J. D. Walecka, "Recent progress in quantum hadrodynamics," *International Journal of Modern Physics E*, vol. 6, no. 4, pp. 515–631, 1997.

[50] W. Bashir, S. Uddin, and R. A. Parra, "Instability of baryonic matter in relativistic mean-field models," *Nuclear Physics A*, vol. 969, pp. 151–172, 2018.

[51] V. Vovchenko, M. I. Gorenstein, and H. Stoceker, "Modeling baryonic interactions with the Clausius-type equation of state," *The European Physical Journal A*, vol. 54, p. 16, 2018.

[52] S. Samanta and B. Mohanty, "Criticality in a hadron resonance gas model with the van der Waals interaction," *Physical Review C*, vol. 97, article 015201, 2018.

[53] The MPD Collaboration, "Status and initial physics performance studies of the MPD experiment at NICA," *The European Physical Journal*, vol. 58, 2022.

[54] V. Vovchenko, M. I. Gorenstein, and H. Stocker, "van der Waals interactions in hadron resonance gas: from nuclear matter to lattice QCD," *Physical Review Letters*, vol. 118, no. 18, p. 182301, 2017.

[55] N. Sarkar and P. Ghosh, "van der Waals hadron resonance gas and QCD phase diagram," *Physical Review C*, vol. 98, no. 1, 2018.

[56] R. Venugopalan and M. Prakash, "Thermal properties of interacting hadrons," *Nuclear Physics A*, vol. 546, pp. 718–760, 1992.

[57] R. K. Mohapatra, H. Mishra, S. Dash, and B. K. Nandi, "Transport coefficients of hadronic matter in a van der Walls hadron resonance gas model," 2019, https://arxiv.org/abs/1901.07238.

[58] C. Eggers and J. Rafelski, "Strangeness and quark gluon plasma: aspects of theory and experiment," *International Journal of Modern Physics A*, vol. 6, pp. 1067–1113, 1991.

[59] S. Uddin and C. P. Singh, "Dependence of $K\pi$ ratio on temperature and chemical potential as a signature of quark gluon plasma," *Physics Letters B*, vol. 278, p. 357, 1992.

[60] J. Sollfrank, M. Gazdzicki, U. Heinz, and J. Rafelski, "Chemical freeze-out conditions in central S-S collisions at 200A GeV," *Zeitschrift für Physik C Particles and Fields*, vol. 61, p. 659, 1994.

[61] J. Letesier, A. Tounsi, U. Heinz, J. Sollfrank, and J. Rafelski, "Strangeness conservation in hot nuclear fireballs," *Physical Review D*, vol. 51, pp. 3408–3435, 1995.

[62] Saeed-Uddin, *Strangeness Production and Thermal Freezeout Conditions in S-S Collisions at 200 GeV* ICTP Preprint No. IC/1995/110.

[63] Saeed-Uddin, "Thermochemical equilibrium and strangeness production at freeze-out in S-S collisions at," *Journal de Physique*, vol. 24, no. 4, pp. 779–789, 1998.

[64] N. A. Maria and D. P. Aspostolos, "Strangeness production in hadronic and quark matter: a quantitative differentiation," *Physical Review D*, vol. 51, pp. 1086–1092, 1995.

[65] S. Uddin, J. S. Ahmad, M. Ali, W. Bashir, R. A. Bhat, and M. Farooq Mir, "Longitudinal hadronic flow at RHIC in extended statistical thermal model and resonance decay effects," *Acta Physica Polonica B*, vol. 41, p. 2633, 2010.

[66] E. Kornas, "Energy dependence of proton and antiproton production in central Pb+Pb collisions from NA49," *The European Physical Journal C*, vol. 49, p. 293, 2007.

[67] F. Becattini, J. Cleymans, and J. Strumpfer, "Rapidity variation of thermal parameters at SPS and RHIC," 2007, https://arxiv.org/pdf/0709.2599.pdf.

[68] F.-H. Liu, Y. Yuan, and M.-Y. Duan, "Net-proton emission in nucleus-nucleus collisions at high energies," *Europhysics Letters*, vol. 81, no. 2, p. 22001, 2008.

[69] J. Cleymans, R. Sahoo, D. P. Mahapatra, D. K. Srivastava, and S. Wheaton, "Saturation of E_T/N_{ch} and freeze-out criteria in heavy-ion collisions," *Journal de Physique*, vol. 35, no. 10, article 104147, 2008.

[70] J. Cleymans, J. Strumpfer, and L. Turko, "Extended longitudinal scaling and the thermal model," *Physical Review C*, vol. 78, article 017901, 2008.

[71] UA5 Collaboration, G. J. Alner, B. Åsman et al., "Scaling of pseudorapidity distributions at c.m. energies up to 0.9 TeV," *Zeitschrift für Physik C Particles and Fields*, vol. 33, no. 1, 1986.

[72] E. Kornasa, "Energy dependence of proton and antiproton production in central Pb+Pb collisions," *The European Physical Journal C*, vol. 49, pp. 293–296, 2007.

[73] NA49 Collaboration, "Energy and centrality dependence of $\bar{p}$ and p production and the $\bar{\Lambda}/\bar{p}$ ratio in Pb+Pb collisions between 20A GeV and 158A GeV," *Physical Review C*, vol. 73, article 044910, 2006.

[74] B. Moskowitz and M. Gonin, "Distributions of transverse energy, protons and mesons from Au+Au collisions at 11.6 A GeV/c," in *Proceedings of XIII Particles and Nuclei, International, Conference (PANIC1 93)*, 1993 Perugia, Italy.

[75] M. Gonin, "Baryon spectra in Au+Au collisions: preliminary results from E-566," in *7th Meeting of the American Physical Society Division of Particles and Fields* FERMILAB, Illinois.

[76] Y. B. Ivanov, "Baryon stopping signal for mixed phase formation in HIC," *Journal of Physics: Conference Series*, vol. 668, article 012061, 2016.

[77] Y. B. Ivanov, "Baryon stopping in heavy-ion collisions at $E_{Lab} = 2 - 160$ GeV/nucleon," *Physics Letters B*, vol. 690, p. 358, 2010.

[78] E. Lavrik, "Compressed baryonic matter experiment at FAIR," *AIP Conference Proceedings*, vol. 2163, article 030009, 2019.

[79] Y. B. Ivanov, "Alternative scenarios of relativistic heavy-ion collisions. I. Baryon stopping," *Physical Review C*, vol. 87, article 064904, 2013.

[80] S. M. H. Wong, "Quantifying baryon stopping in high energy nuclear collisions," *Physics Letters B*, vol. 480, p. 65, 2000.

[81] M. Michalec, "Thermal description of particle production in ultra-relativistic heavy-ion collisions," 2001, https://arxiv.org/abs/nucl-th/0112044.

[82] S. Chatterjee, S. Das, K. Lokesh et al., "Freeze-out parameters in heavy-ion collisions at AGS, SPS, RHIC, and LHC energies," *Advances in High Energy Physics*, vol. 2015, Article ID 349013, 20 pages, 2015.

[83] M. Hadrons, *Boiling quarks–from Hagedorn temperature to ultra-relativistic heavy-ion collisions at CERN*, Johann Rafelski, 2016.

[84] C. Alt, T. Anticic, B. Baatar et al., "Energy dependence of Λ and Ξ production in central Pb+Pb collisions at 20A,30A,40A,80A, and 158A GeV measured at the CERN Super Proton Synchrotron," *Physical Review C*, vol. 78, article 034918, 2008.

[85] C. Meurer and NA49 Collaboration, "Xi and AntiXi production in Pb+Pb collisions at 40A GeV at CERN SPS," *J. Phys. G*, vol. 30, pp. S175–S180, 2004.

[86] T. Kollegger and for the NA49 Collaboration, "Energy dependence of kaon production in central Pb+Pb collisions," *Journal de Physique*, vol. 28, no. 7, pp. 1689–1695, 2002.

[87] J. Manninen, F. Becattini, A. Keränen, M. Gaździcki, and R. Stock, "Study on chemical equilibrium in nucleus-nucleus collisions at relativistic energies," *Acta Physica Hungarica*, vol. 24, no. 1-4, pp. 23–29, 2005.

[88] Y. Aoki, Z. Fodor, S. D. Katz, and K. K. Szabo, "The QCD transition temperature: results with physical masses in the continuum limit," *Physics Letters B*, vol. 643, pp. 46–54, 2006.

[89] Y. Aoki, G. Endrodi, Z. Fodor, S. D. Katz, and K. K. Szabo, "The order of the quantum chromodynamics transition predicted by the standard model of particle physics," *Nature*, vol. 443, no. 7112, pp. 675–678, 2006.

[90] STAR Collaboration, "An experimental exploration of the QCD phase diagram: the search for the critical point and the onset of de-confinement," 2010, https://arxiv.org/abs/1007.2613.

[91] HotQCD Collaboration, "Equation of state in (2+1)-flavor QCD," *Physical Review D*, vol. 90, article 094503, 2014.

[92] H. Caines, "The search for critical behavior and other features of the QCD phase diagram–current status and future prospects," *Nuclear Physics A*, vol. 967, pp. 121–128, 2017.

[93] A. Bazavov, H.-T. Ding, P. Hegde et al., "QCD equation of state to $O(\mu_B^6)$ from lattice QCD," *Physical Review D*, vol. 95, no. 5, article 054504, 2017.

[94] S. Ejiri, "Canonical partition function and finite density phase transition in lattice QCD," *Physical Review D*, vol. 78, article 074507, 2008.

[95] E. S. Bowman and J. I. Kapusta, "Critical points in the linear σ model with quarks," *Physical Review C*, vol. 79, article 015202, 2009.

[96] M. A. Stephanov, "QCD phase diagram and the critical point," *Progress of Theoretical Physics Supplement*, vol. 153, pp. 139–156, 2004.

[97] A. Ayala, B. A. Zamora, J. J. Cobos-Martinez et al., "Plasma screening and the critical end point in the QCD phase diagram," 2022, https://arxiv.org/abs/2208.08590.

[98] S. Sharma, "The QCD equation of state and critical end-point estimates at $O(\mu_B^6)$," *Nuclear Physics A*, vol. 967, pp. 728–731, 2017.

[99] S. Borsányi, Z. Fodor, J. N. Guenther et al., "Lattice QCD equation of state at finite chemical potential from an alternative expansion scheme," *Physical Review Letters*, vol. 126, no. 23, article 232001, 2021.

[100] STAR White Paper (STAR Collaboration), *Studying the Phase Diagram of QCD Matter at RHIC*, 2014.

[101] S. K. Tiwari and C. P. Singh, "Particle production in ultrarelativistic heavy-ion collisions: a statistical- thermal model review," *Advances in High Energy Physics*, vol. 2013, Article ID 805413, 27 pages, 2013.

[102] J. Cleymans, H. Oeschler, K. Redlich, and S. Wheaton, "Comparison of chemical freeze-out criteria in heavy-ion collisions," *Physical Review C*, vol. 73, article 034905, 2006.

[103] R. A. Parra, S. Uddin, W. Bashir, and I.-u. Bashir, "Particle ratios in a multi component non-ideal hadron resonance gas," https://arxiv.org/abs/1912.08134.